Understanding the Iron Absorption Signal of the Ultra-Hot Jupiter WASP-76b Using 3D Modelling Techniques

Joost P. Wardenier – Department of Physics, University of Oxford, UK

Collaborators – Vivien Parmentier (Oxford), Elsie K.H. Lee (Bern), Michael R. Line (ASU), Ehsan Gharib-Nezhad (NASA Ames)

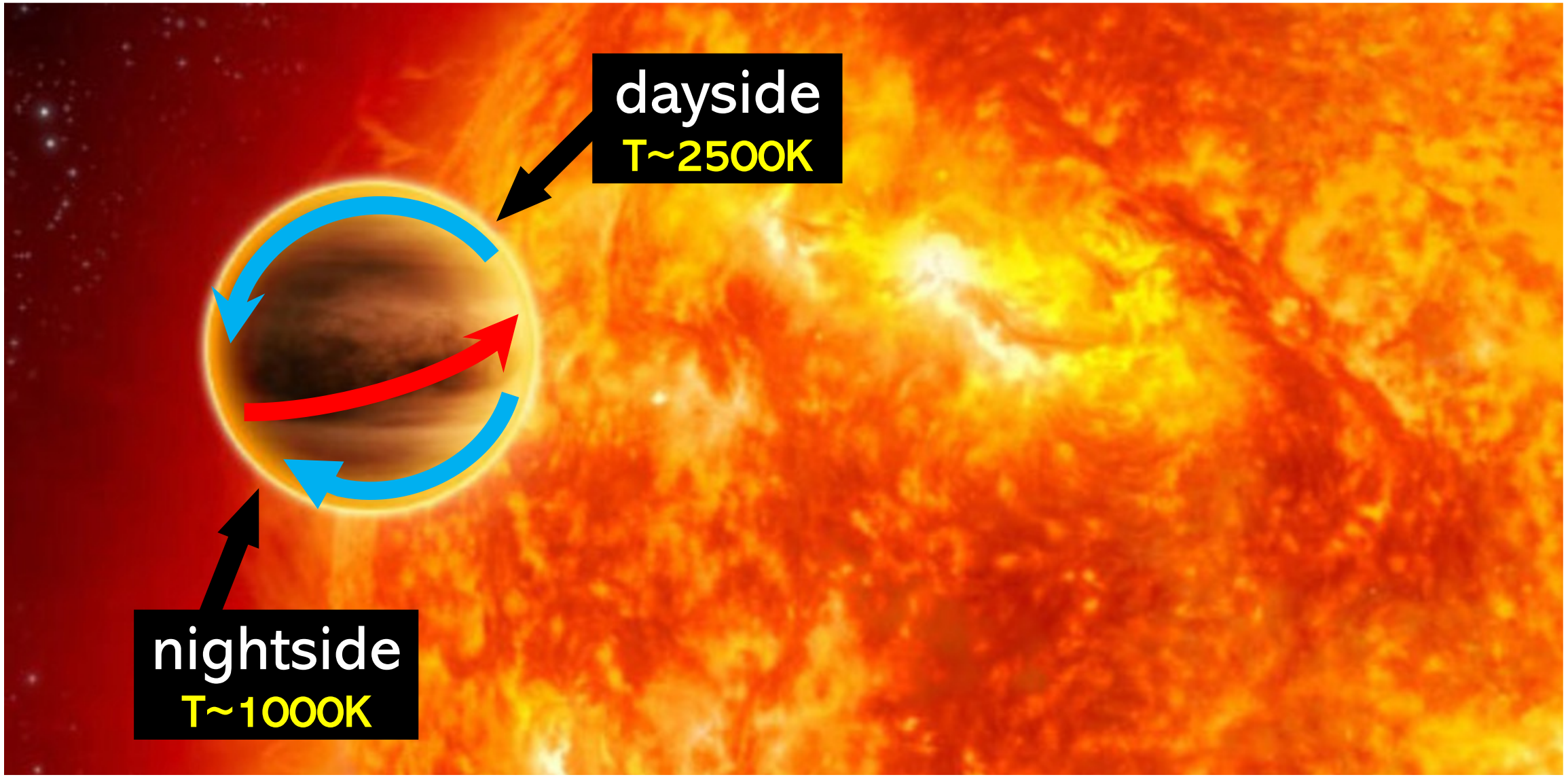

Credit: C. Carreau / ESA

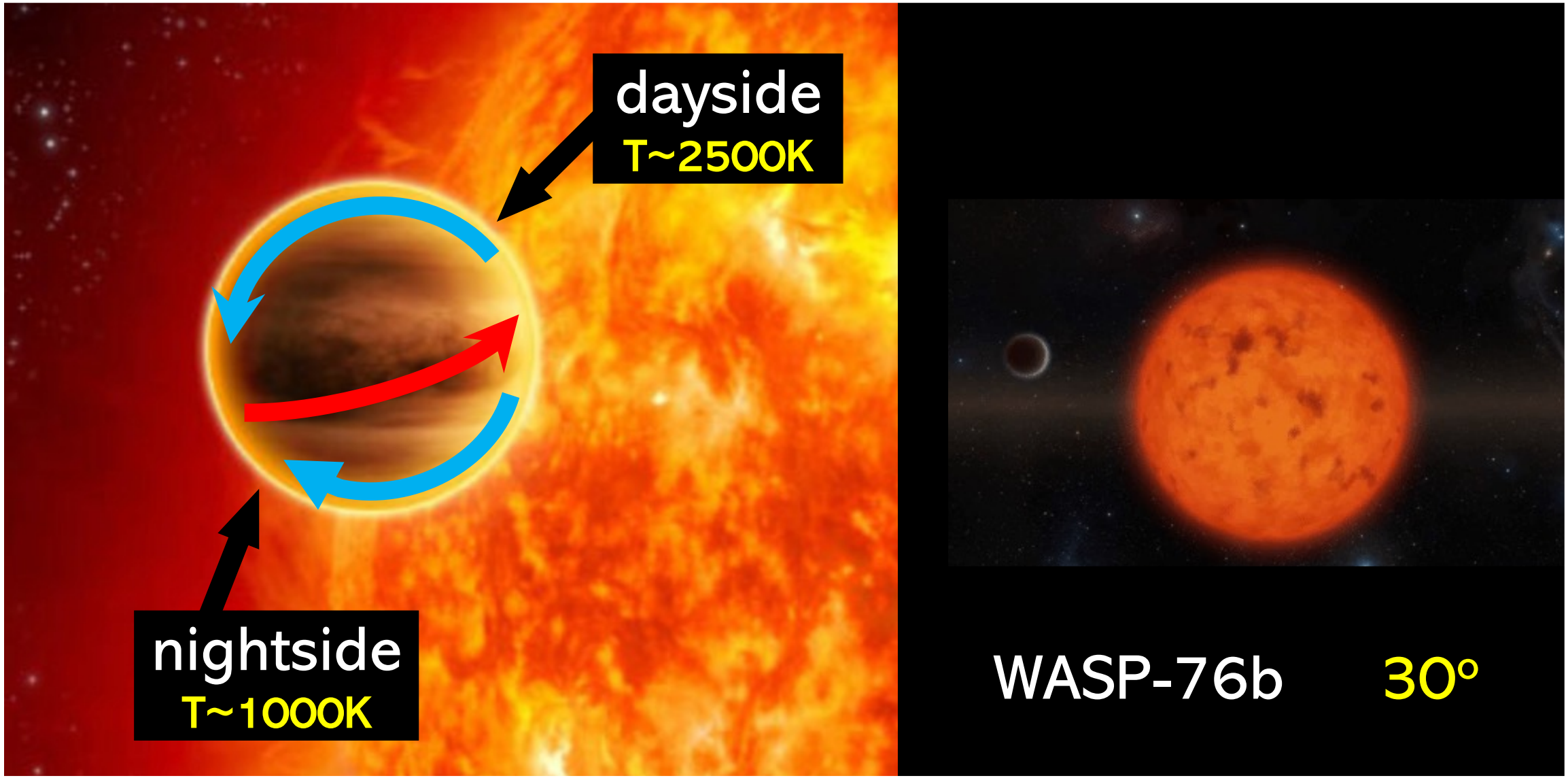

Credit: C. Carreau / ESA

Credit: NASA JPL

High-Resolution Spectroscopy

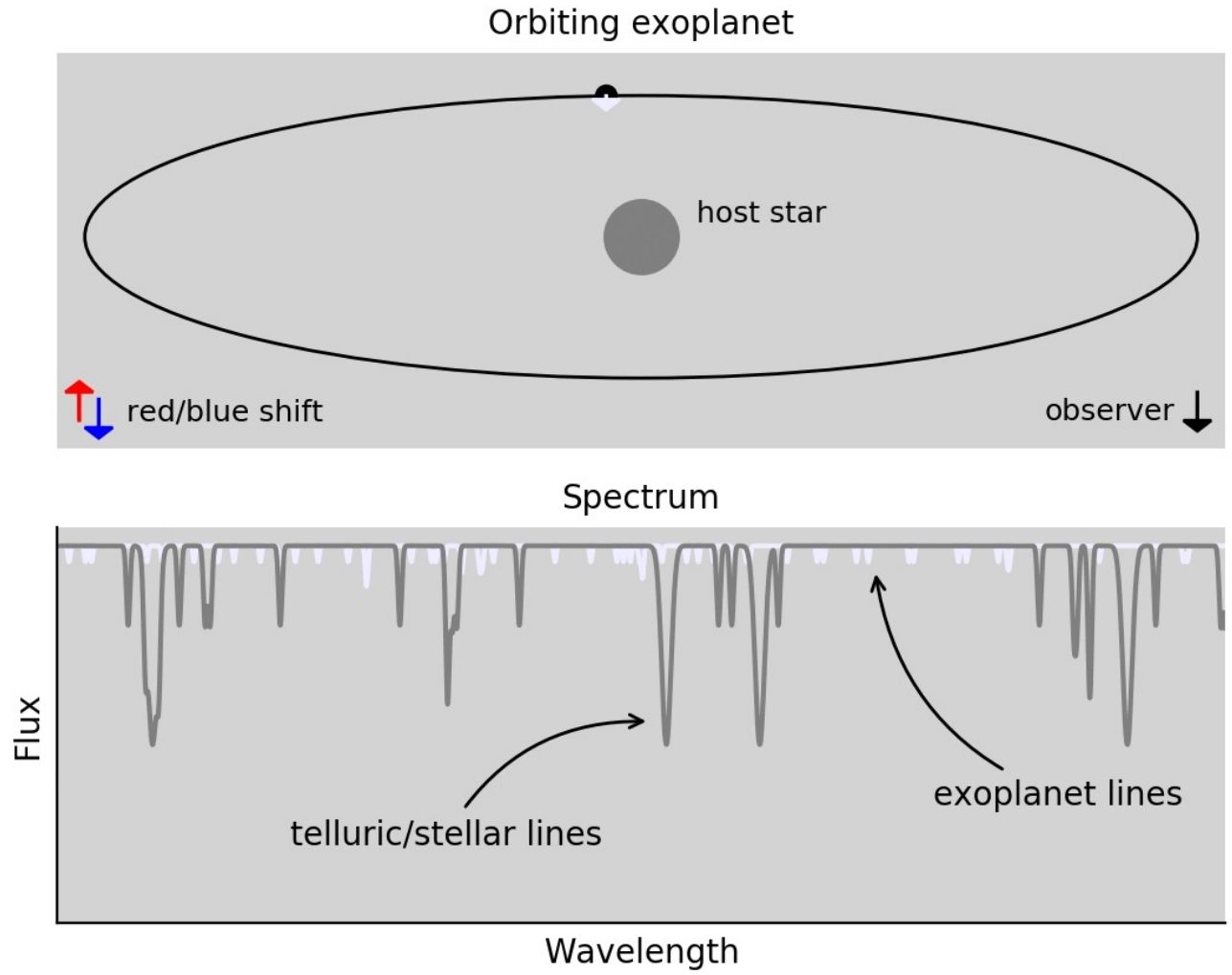

Animation by Lennart van Sluijs

High-Resolution Spectroscopy

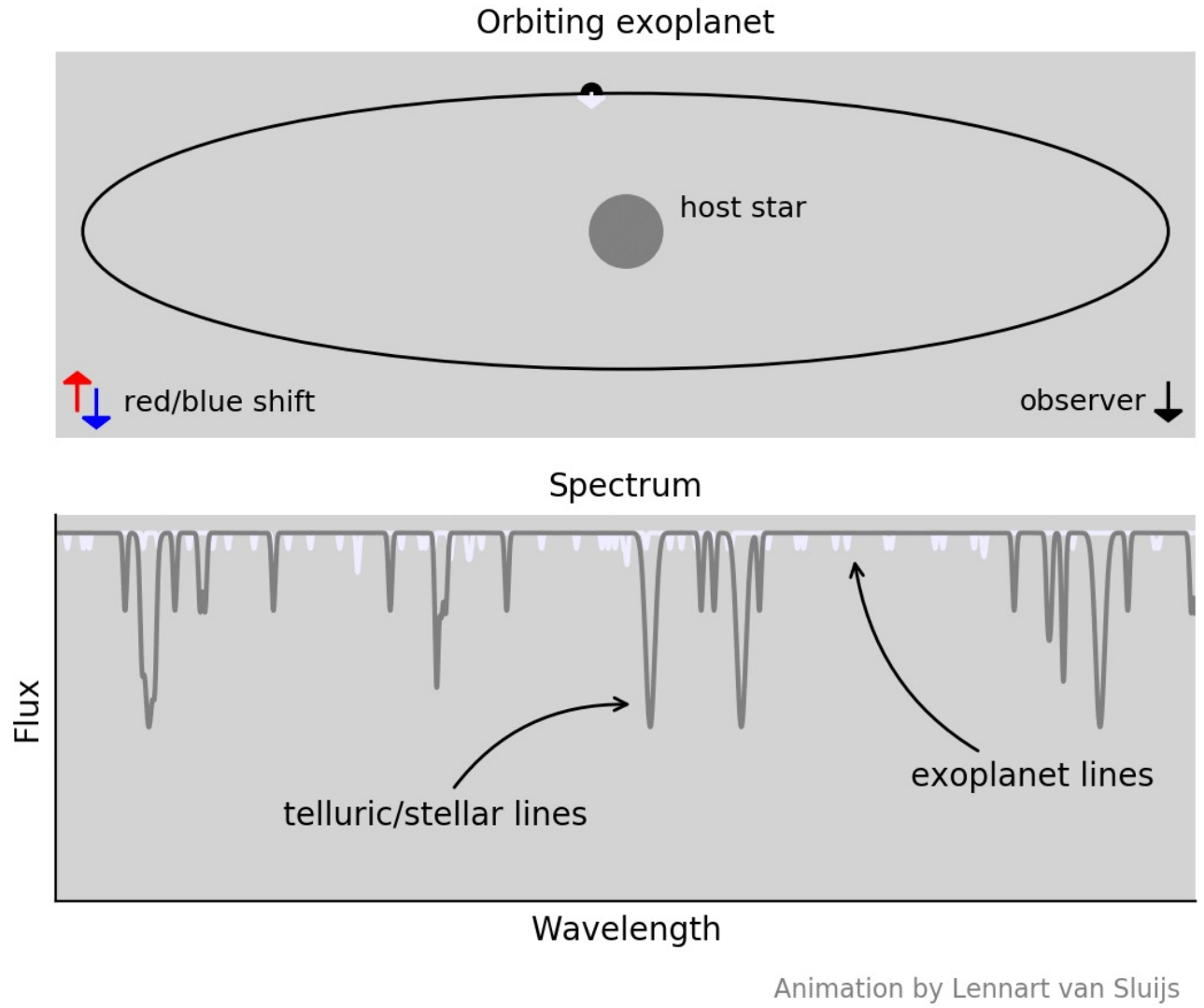

Animation by Lennart van Sluijs

Sources of Doppler shift:

- Systemic velocity
- Orbital velocity
- Planetary rotation
- Winds

Planetary rest frame

The Cross-Correlation Technique

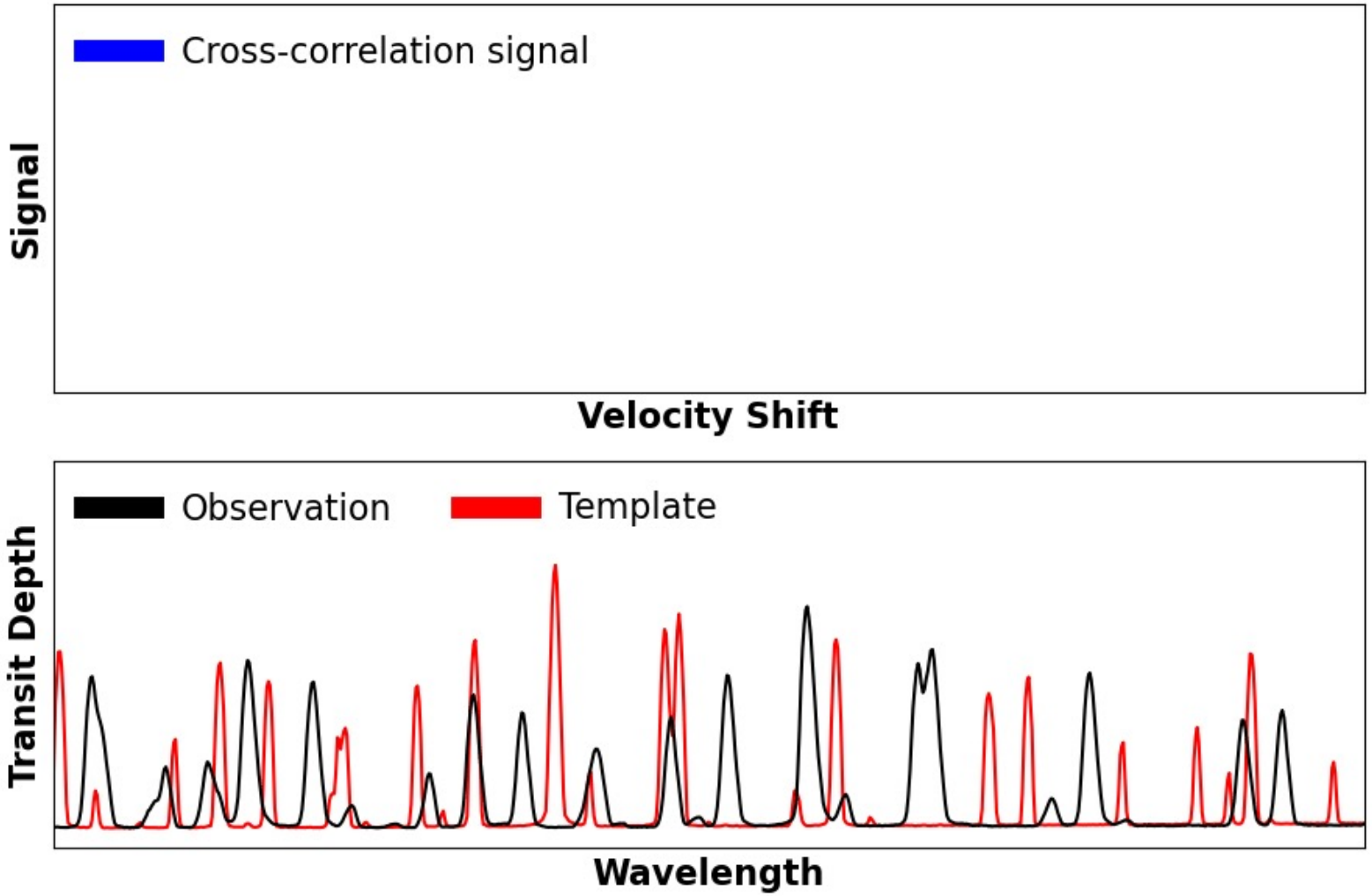

WASP-76b Iron Signal

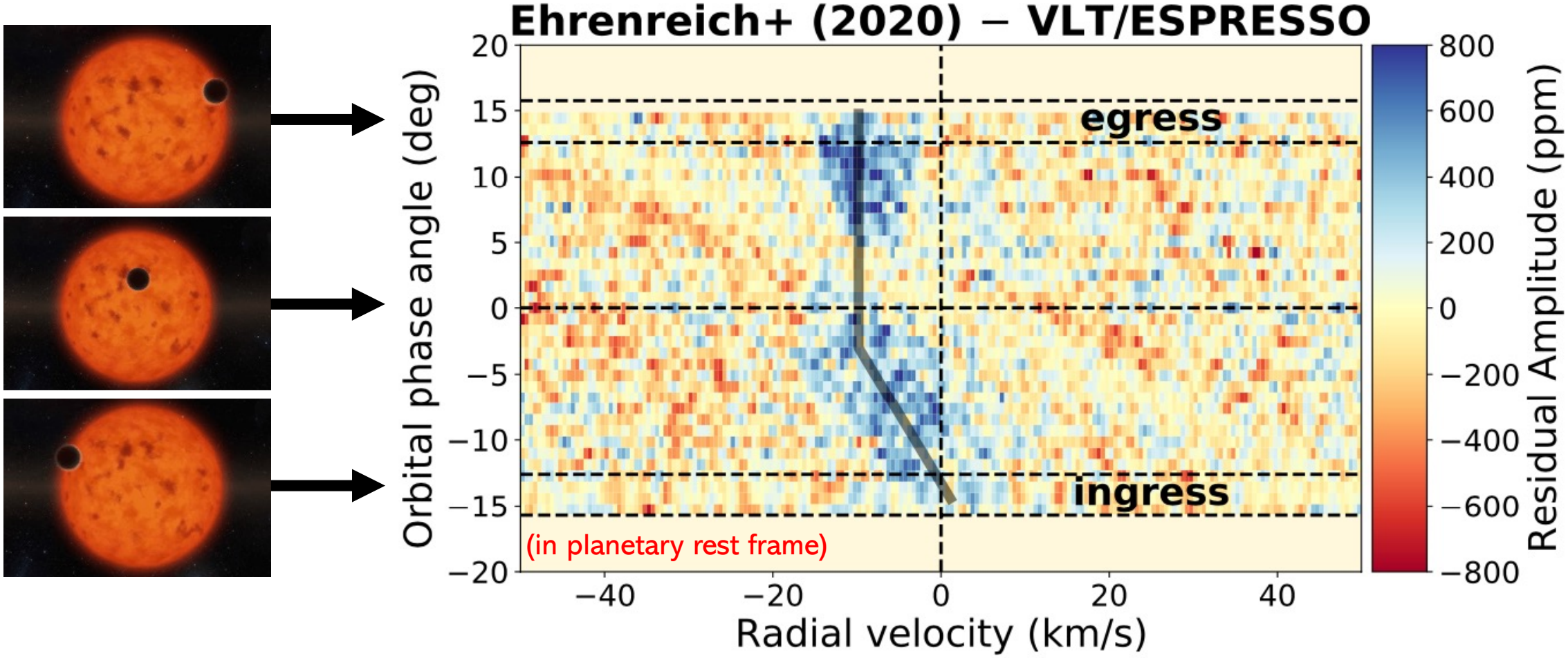

(signal verified by Kesseli & Snellen 2021 with HARPS)

Liquid iron rain spotted on super-heated exoplanet WASP-76b

SPACE 11 March 2020

On This Scorching-Hot Exoplanet, a Forecast of Molten Iron Rain

Winds on WASP-76b blow gaseous iron into cooler regions, where it condenses and falls to the planet's surface as liquid

Science & Environment

Wasp-76b: The exotic inferno planet where it 'rains iron'

Scientists identify rain of molten iron on distant exoplanet

Conditions on Wasp-76b in Pisces include temperatures of 2,400C and 10,000mph winds

HOT IN HERE Toxic 2,400C 'hell planet' Wasp-76b that rains liquid iron found – and it would vaporise you instantly

Cloudy with a chance of metal: Ultra-hot exoplanet where it rains iron observed

TECH & SCIENCE

Iron Rain May Fall on This Scorching-Hot Exoplanet Where Temperatures Reach More Than 4,000 Degrees

NEWS ASTRONOMY

Heavy metal may rain from the skies of planet WASP 76b

Astronomers observed evidence of iron rain on the ultrahot gas giant

Good luck pitching a tent on exoplanet WASP-76b, the bloody raindrops here are made out of molten iron

Raining iroooooon, from a lacerated sky

Molten iron rain falls through the skies of scorching-hot exoplanet

WASP-76b Iron Signal

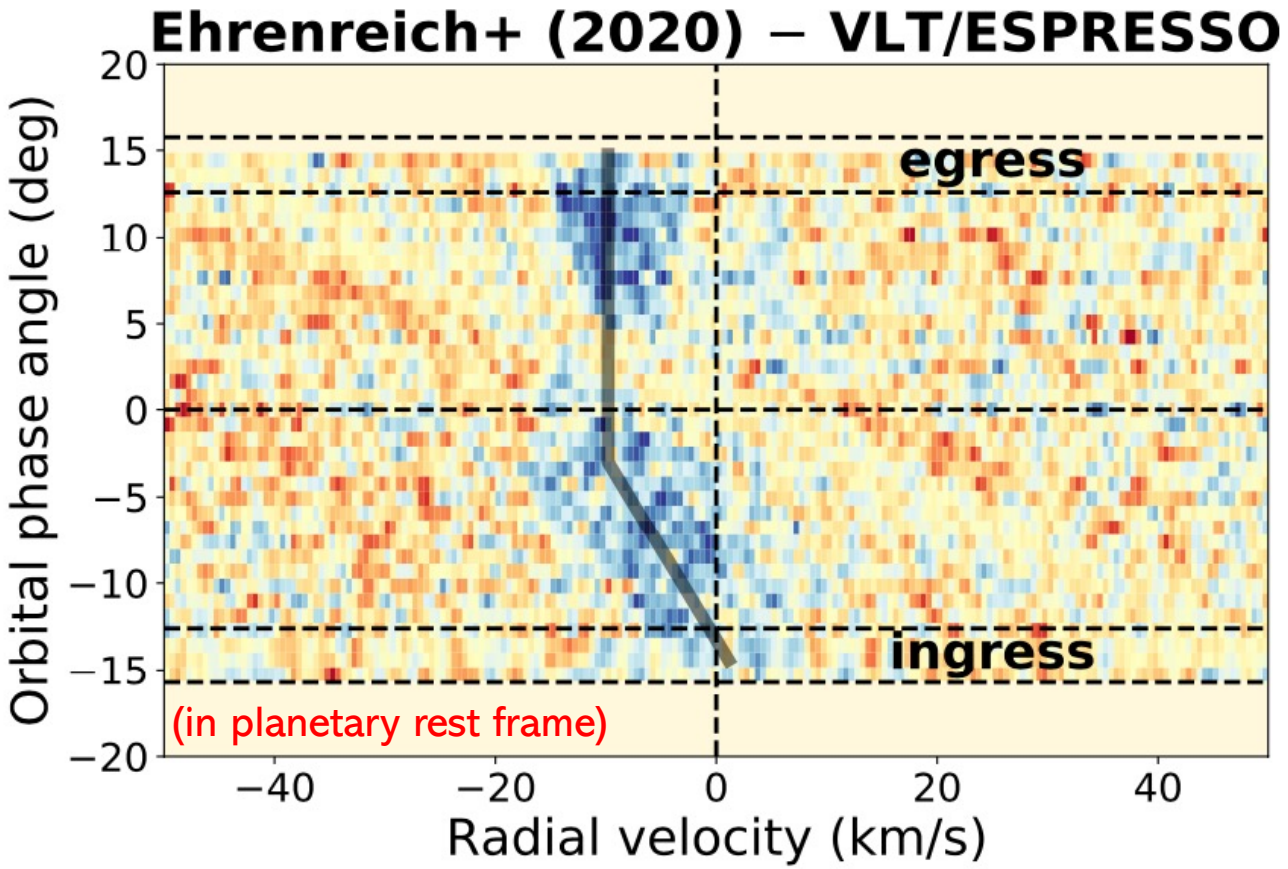

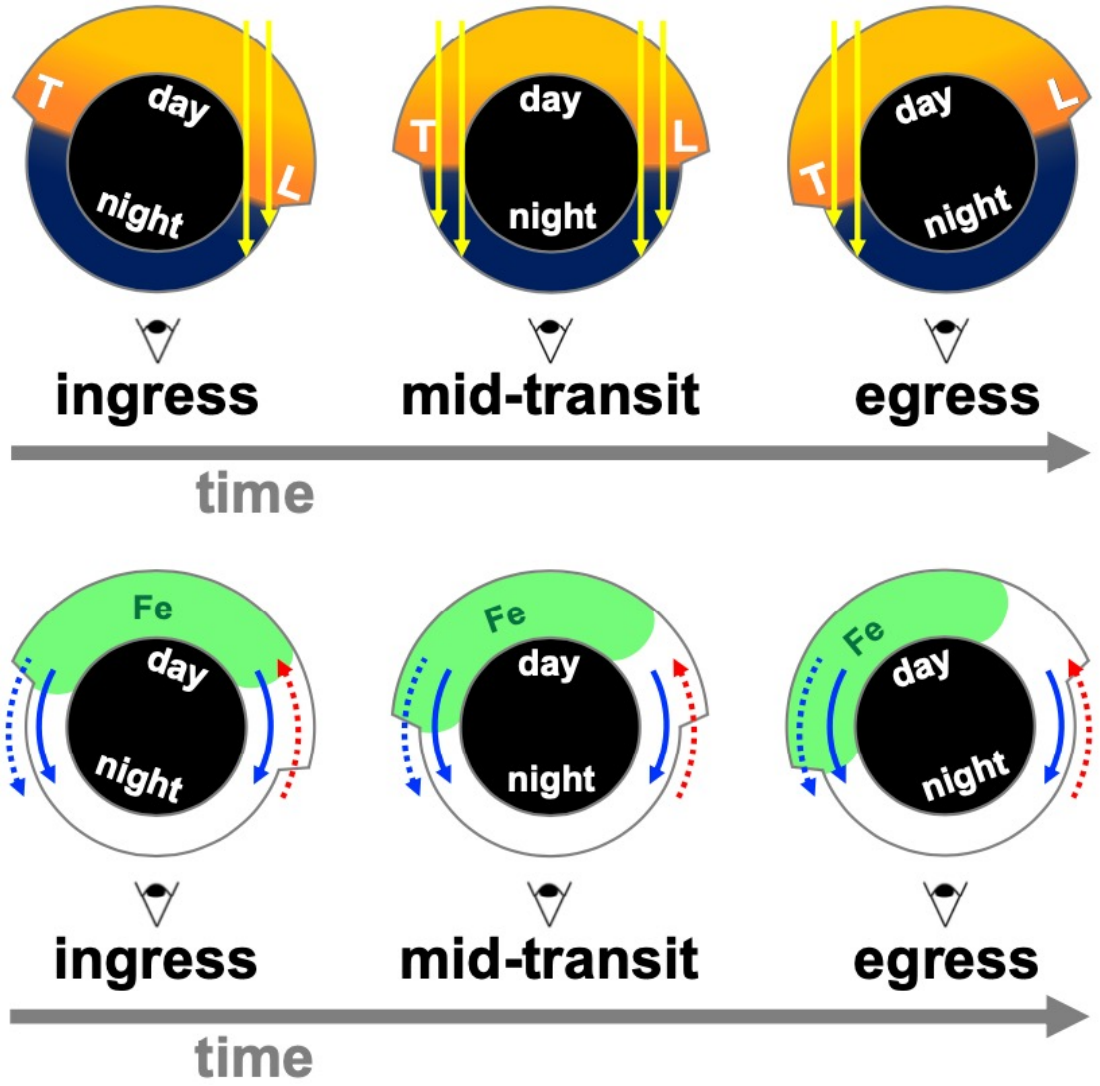

How do 3D effects* influence the iron absorption signal of ultra-hot Jupiters in transmission?

* Spatial variations in temperature, chemistry, wind speed, scale height, irradiation, etc.

3D Monte-Carlo Radiative Transfer

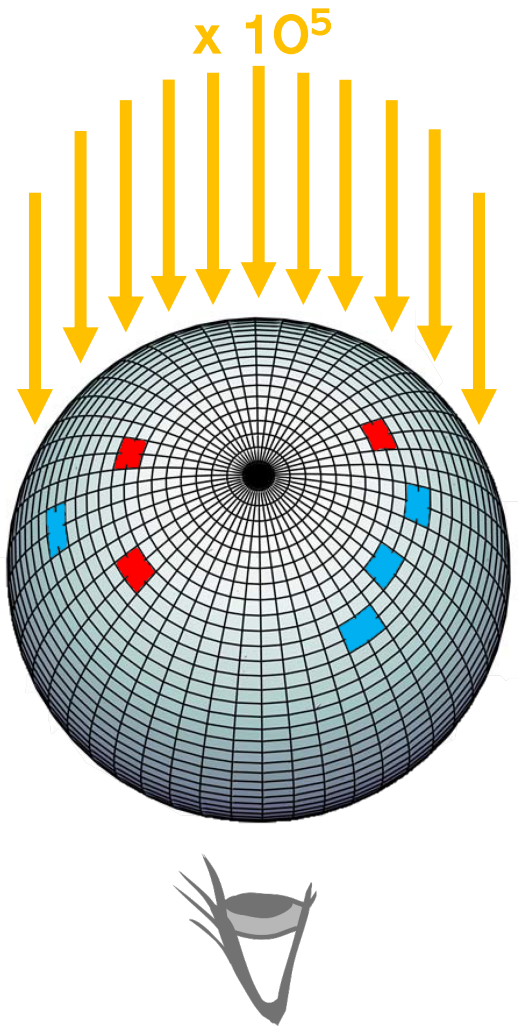

Global Circulation Model (SPARC/MITgcm)

Showman+ 2009 (ApJ)

↓

Monte-Carlo Radiative Transfer (hires-MCRT)

Adapted from Lee+ 2017, 2019 (MNRAS)

↓

Transmission spectra

↓

Cross-Correlation map

Equatorial plane

Temperature structure

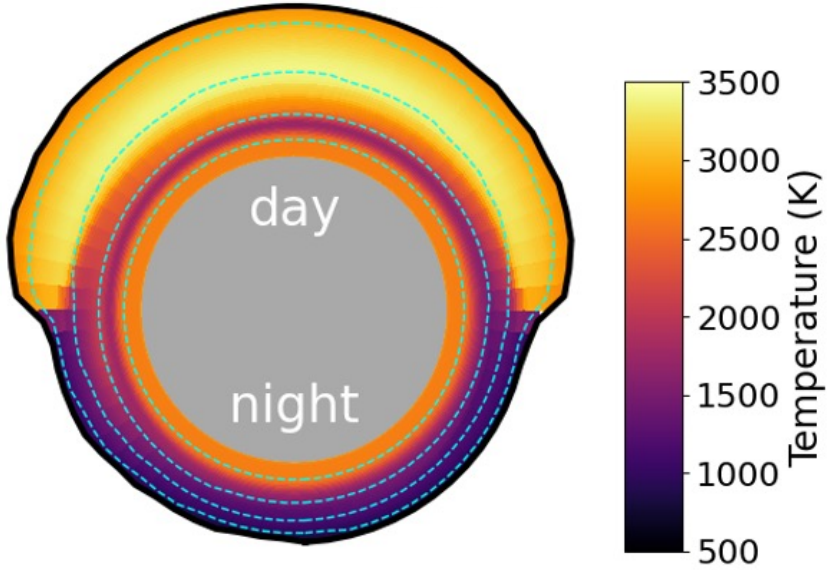

Iron abundances

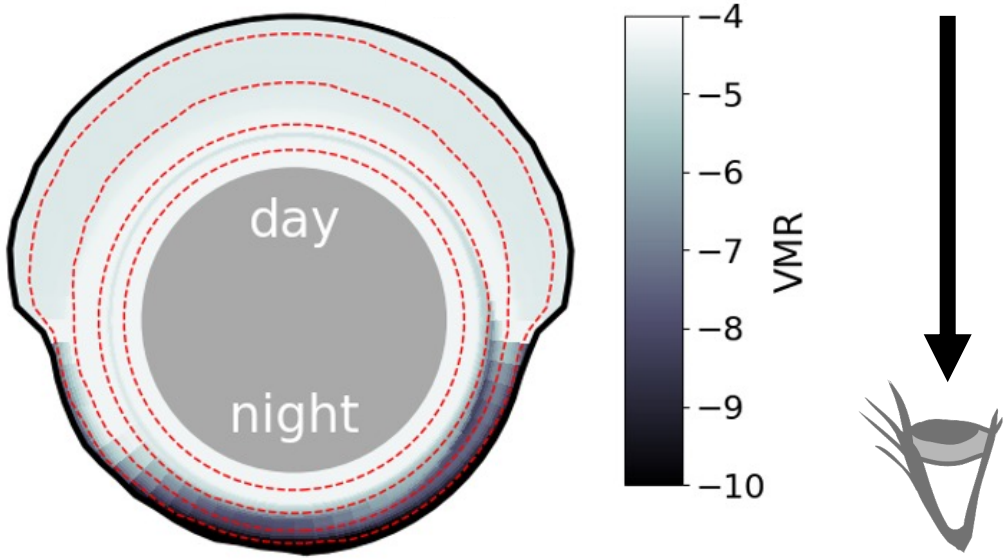

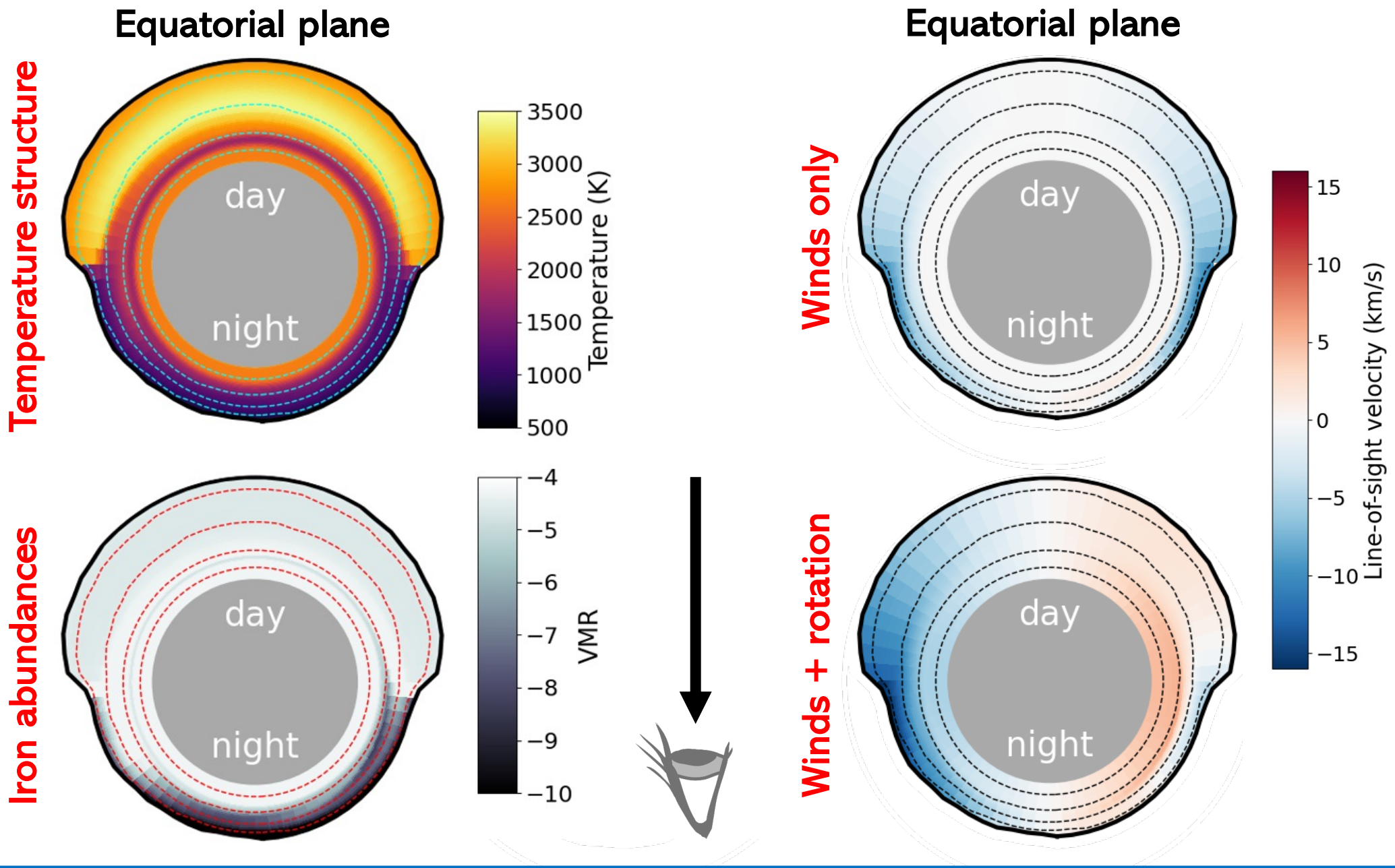
Equatorial plane
Equatorial plane
Temperature structure
Winds only
Iron abundances
Winds + rotation
day
night
day
night
day
night
day
night
3500
3000
2500
2000
1500
1000
500
Temperature (K)
−4
−5
−6
−7
−8
−9
−10
VMR
15
10
5
0
−5
−10
−15
Line-of-sight velocity (km/s)

Time-Dependent Spectra

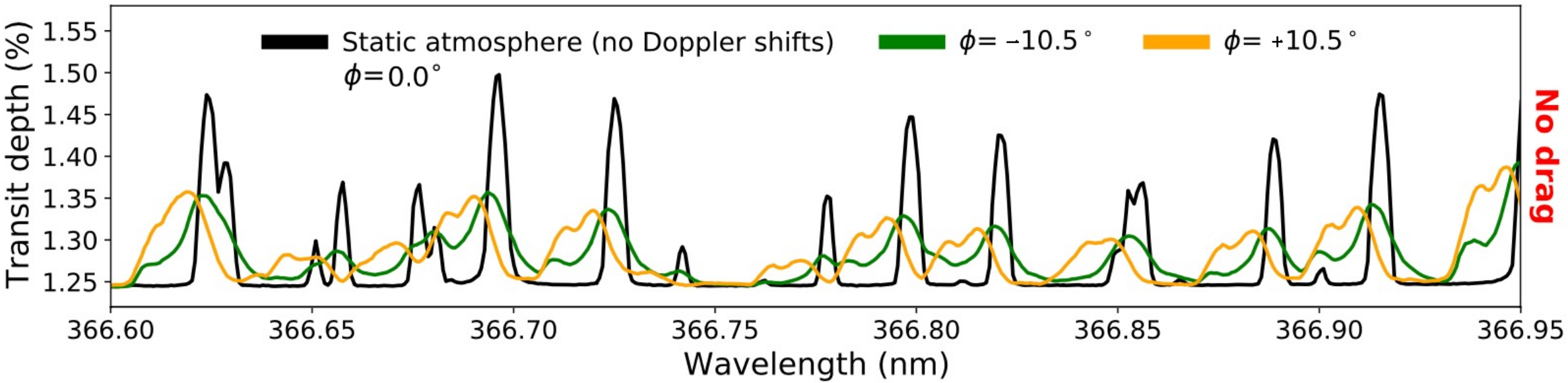

Time-Dependent Spectra

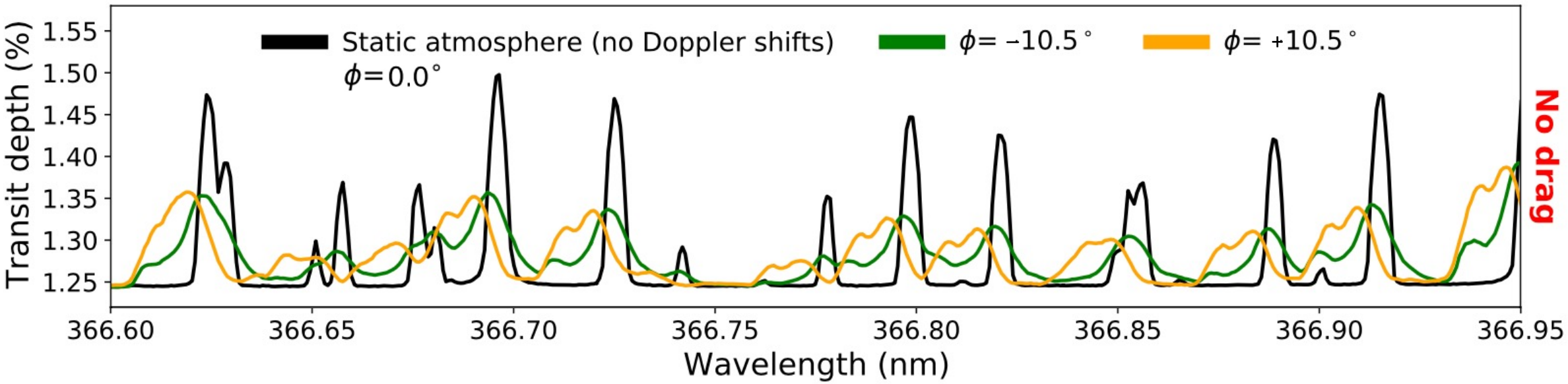

- Spatial distribution of iron
- 3D temperature structure
- Atmospheric dynamics
- Planetary rotation

→

- Line position
- Line shape
- Line depth

(time-dependent)

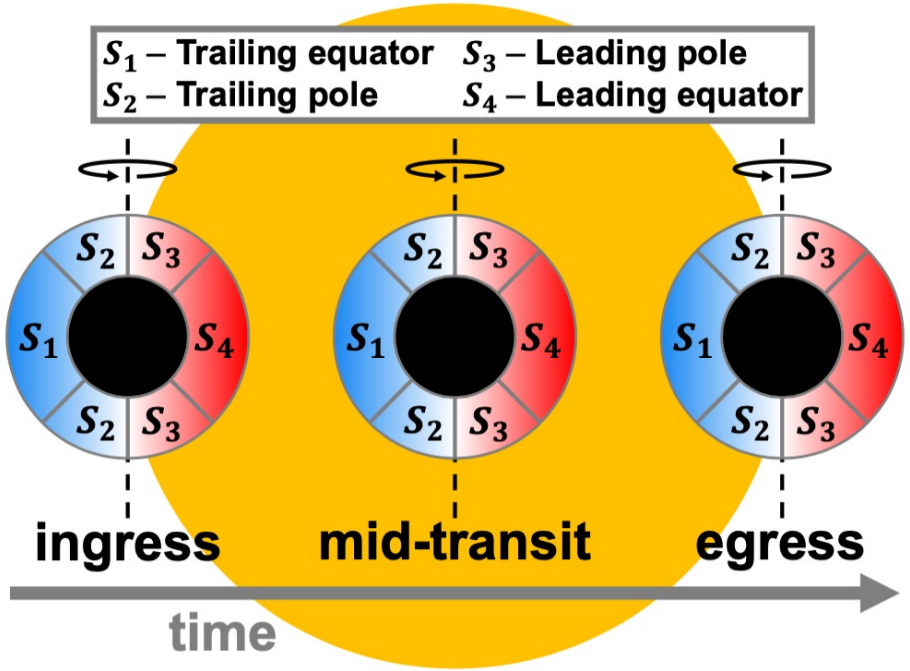
S_1 – Trailing equator
S_2 – Trailing pole
S_3 – Leading pole
S_4 – Leading equator
S_2 S_3 S_1 S_4 S_2 S_3
S_2 S_3 S_1 S_4 S_2 S_3
S_2 S_3 S_1 S_4 S_2 S_3
ingress
mid-transit
egress
time

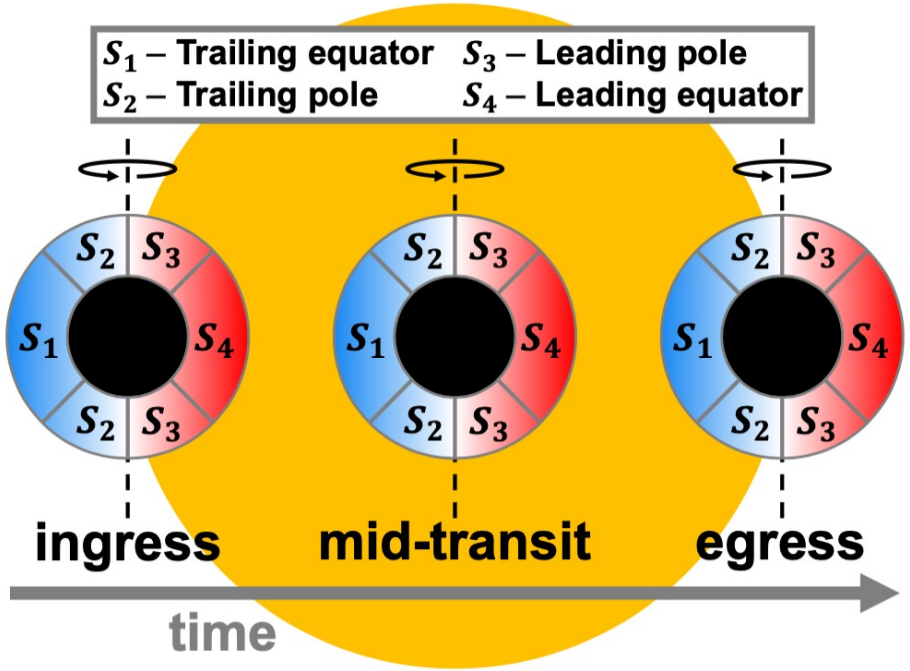
S_1 – Trailing equator
S_2 – Trailing pole
S_3 – Leading pole
S_4 – Leading equator
S_1 S_2 S_3 S_4
ingress
mid-transit
egress
time

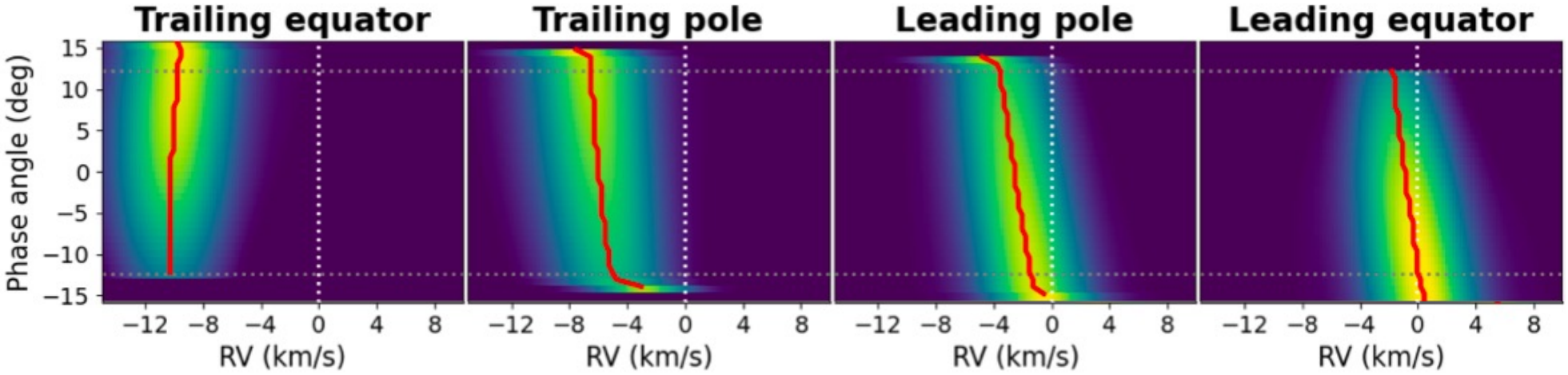
Trailing equator
Trailing pole
Leading pole
Leading equator
Phase angle (deg)
15
10
5
0
−5
−10
−15
−12 −8 −4 0 4 8
RV (km/s)

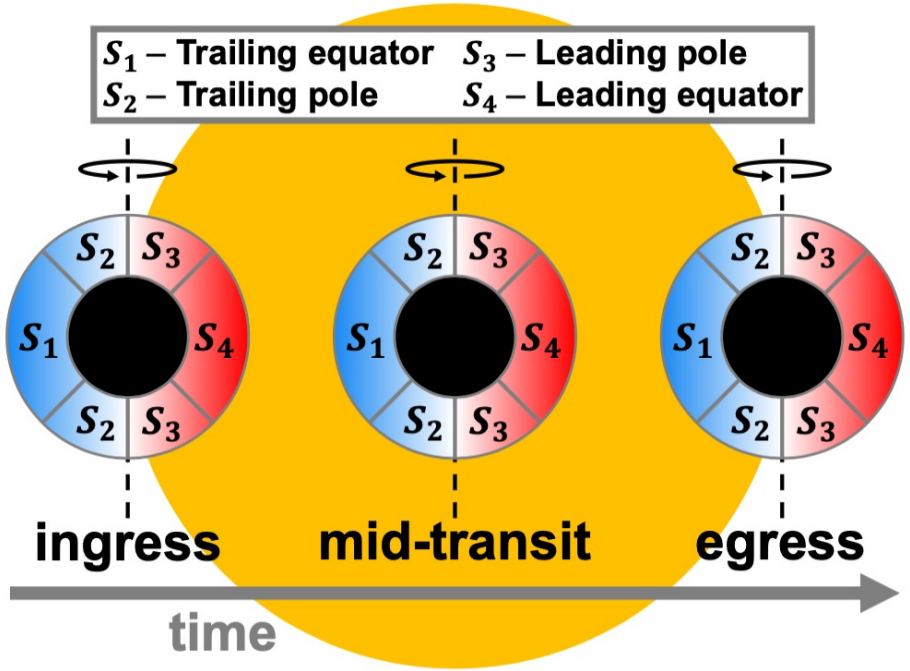
S_1 – Trailing equator
S_2 – Trailing pole
S_3 – Leading pole
S_4 – Leading equator
ingress
mid-transit
egress
time

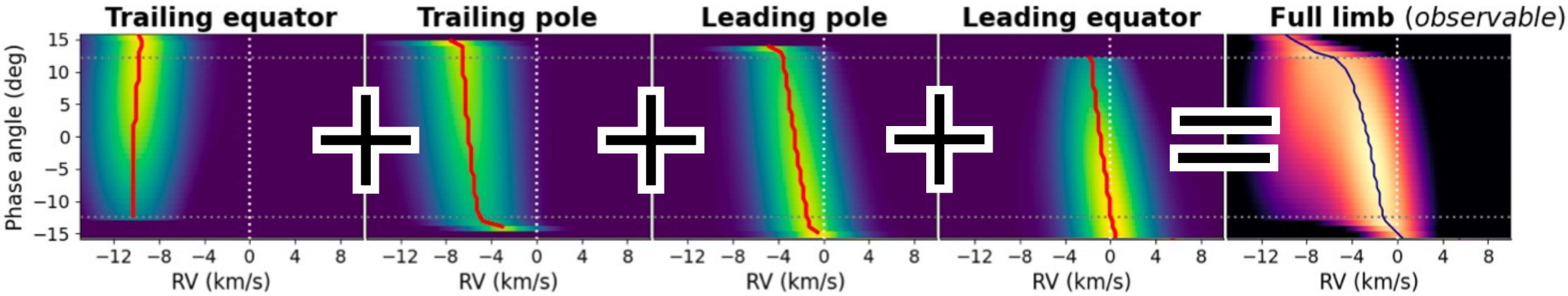
Trailing equator
Trailing pole
Leading pole
Leading equator
Full limb (observable)
Phase angle (deg)
RV (km/s)

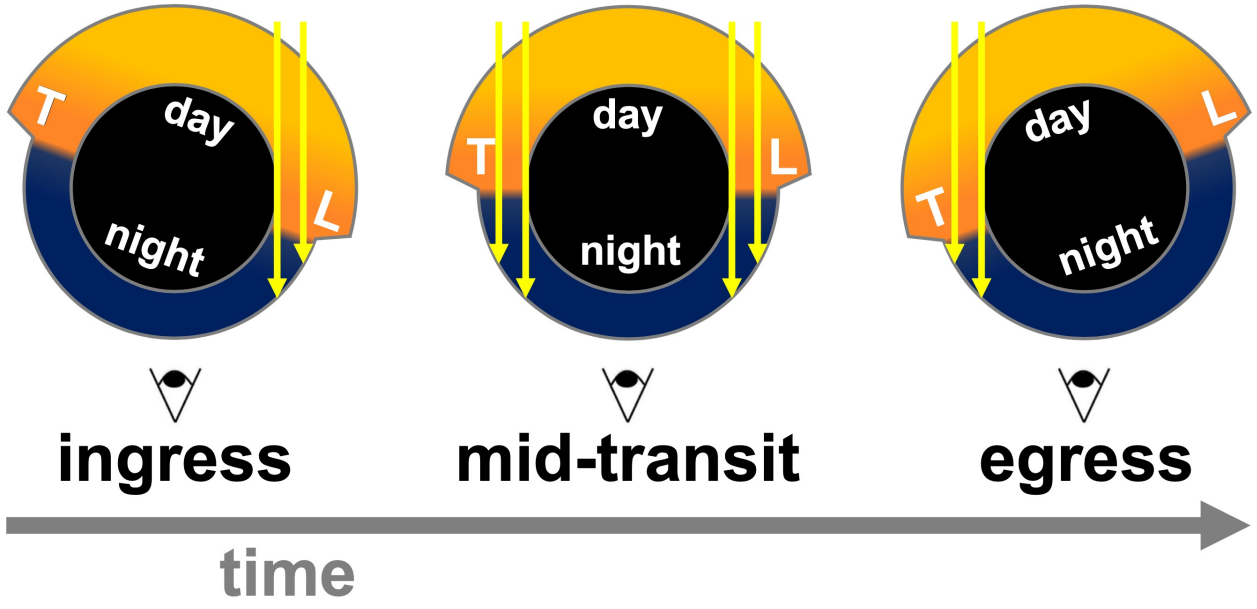
T
day
night
L
ingress
mid-transit
egress
time

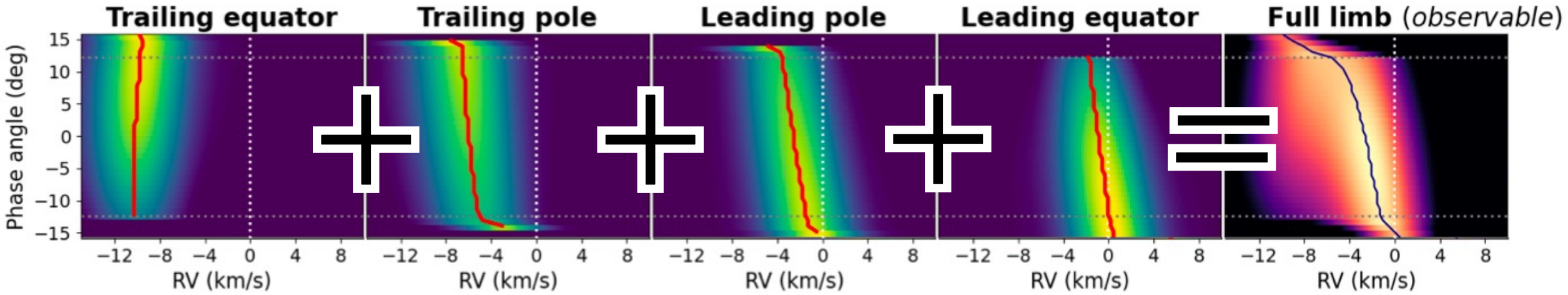
Trailing equator
Trailing pole
Leading pole
Leading equator
Full limb (observable)
Phase angle (deg)
15
10
5
0
−5
−10
−15
−12 −8 −4 0 4 8
RV (km/s)

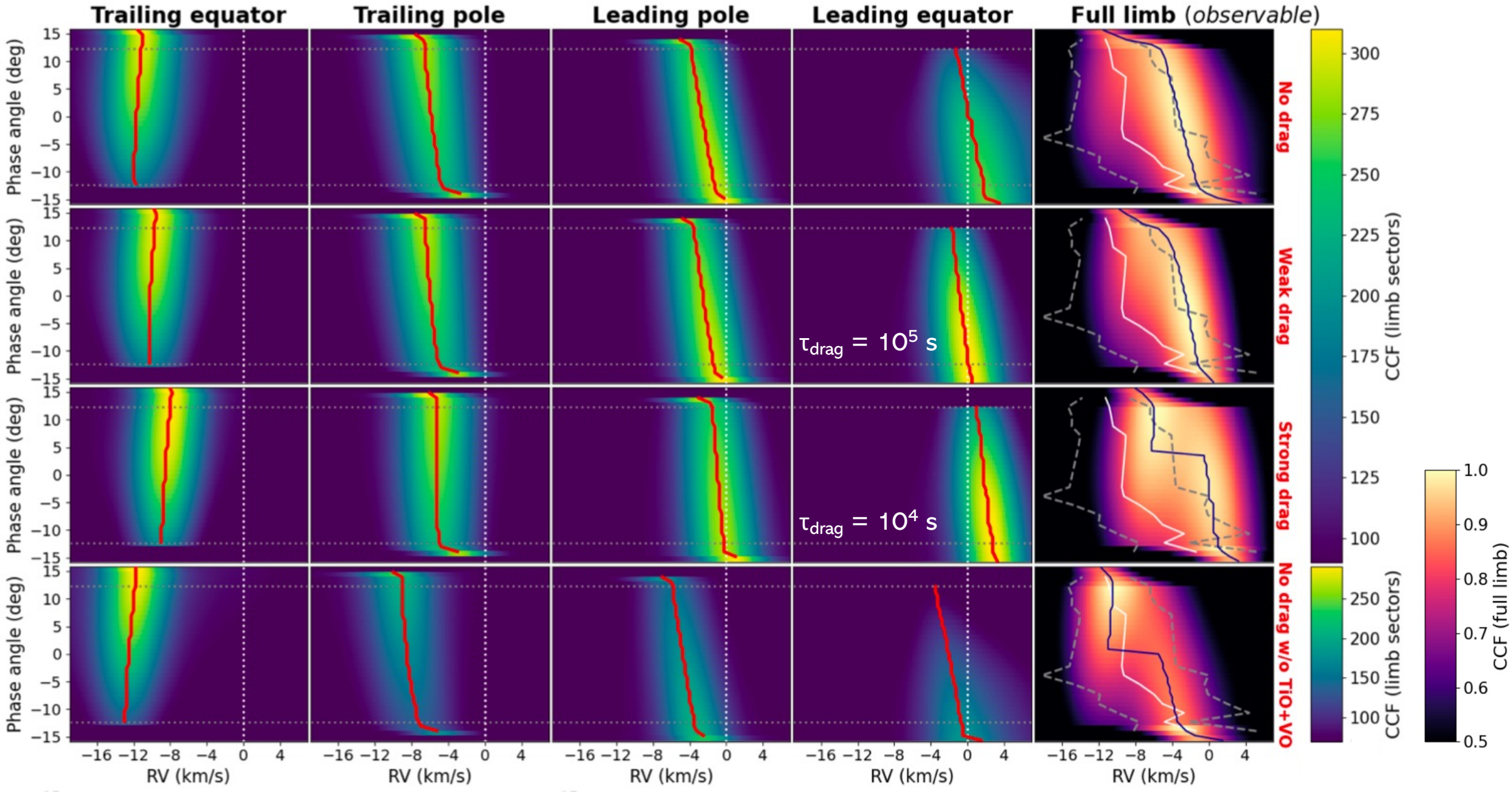
Trailing equator
Trailing pole
Leading pole
Leading equator
Full limb (observable)
Phase angle (deg)
RV (km/s)
No drag
Weak drag
Strong drag
No drag w/o TiO+VO
τdrag = 10^5 s
τdrag = 10^4 s
CCF (limb sectors)
CCF (full limb)

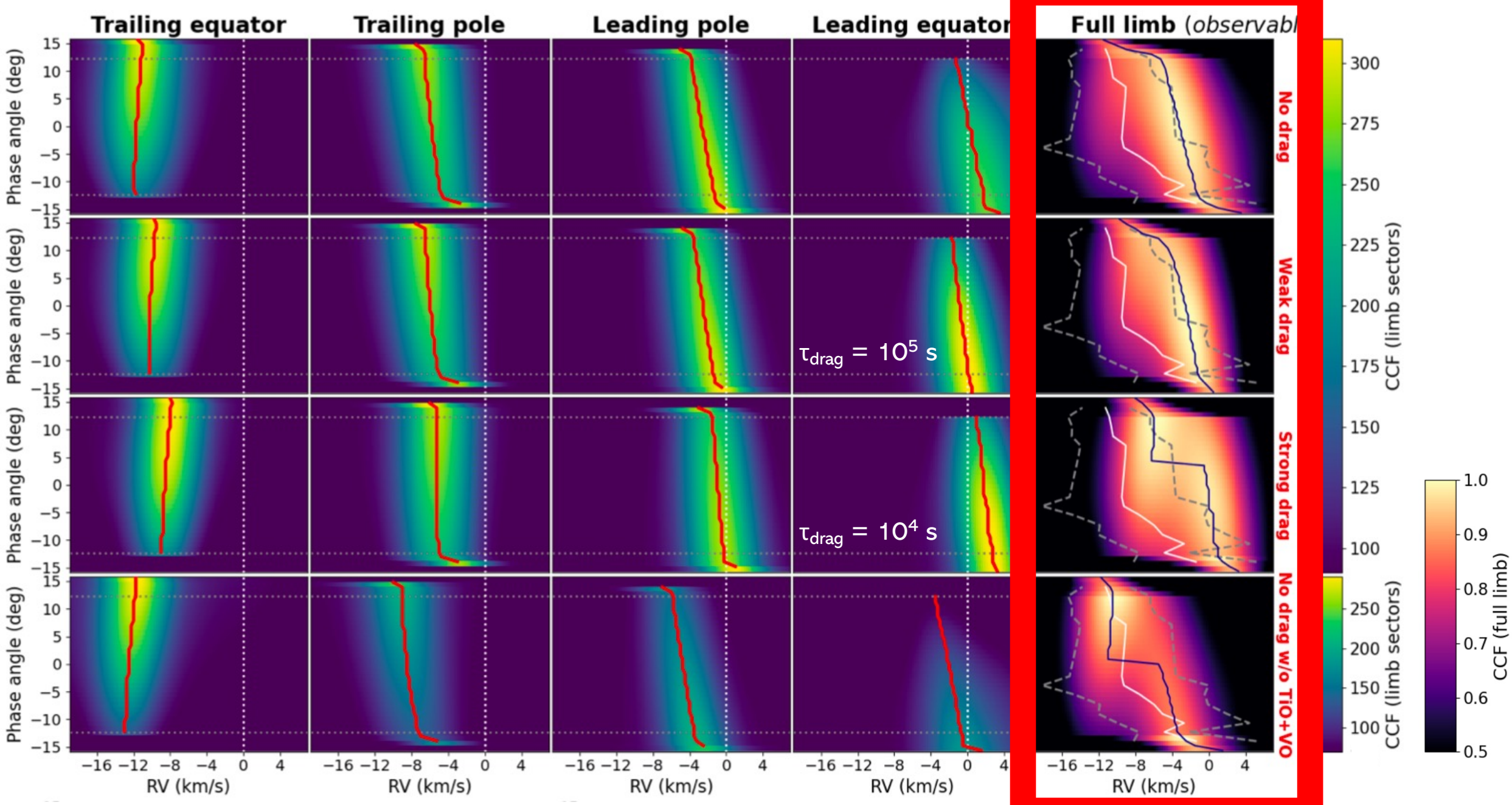
Trailing equator
Trailing pole
Leading pole
Leading equator
Full limb (observabl
Phase angle (deg)
RV (km/s)
No drag
Weak drag
Strong drag
No drag w/o TiO+VO
τdrag = 10^5 s
τdrag = 10^4 s
CCF (limb sectors)
CCF (full limb)

Nightside temperatures on leading limb

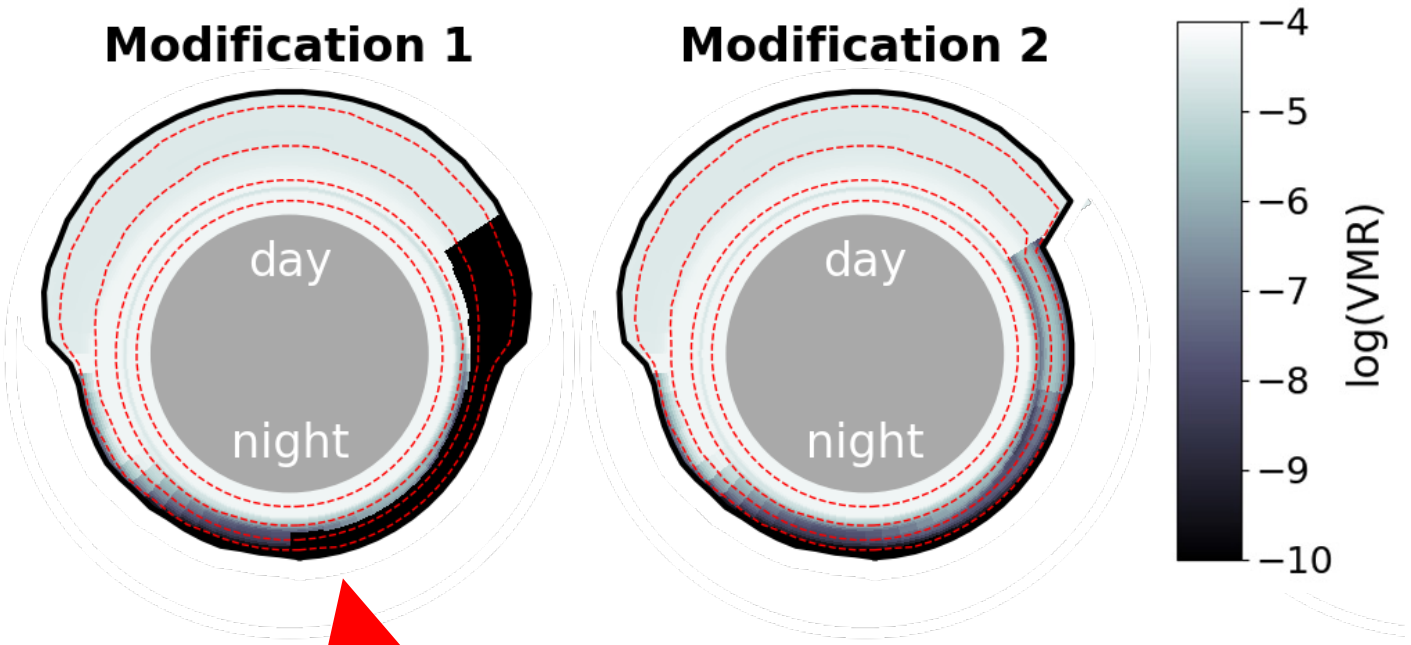

Iron removed from leading limb

Nightside temperatures on leading limb

Intermediate temperature on leading limb (1800K)
+ uniform iron abundances

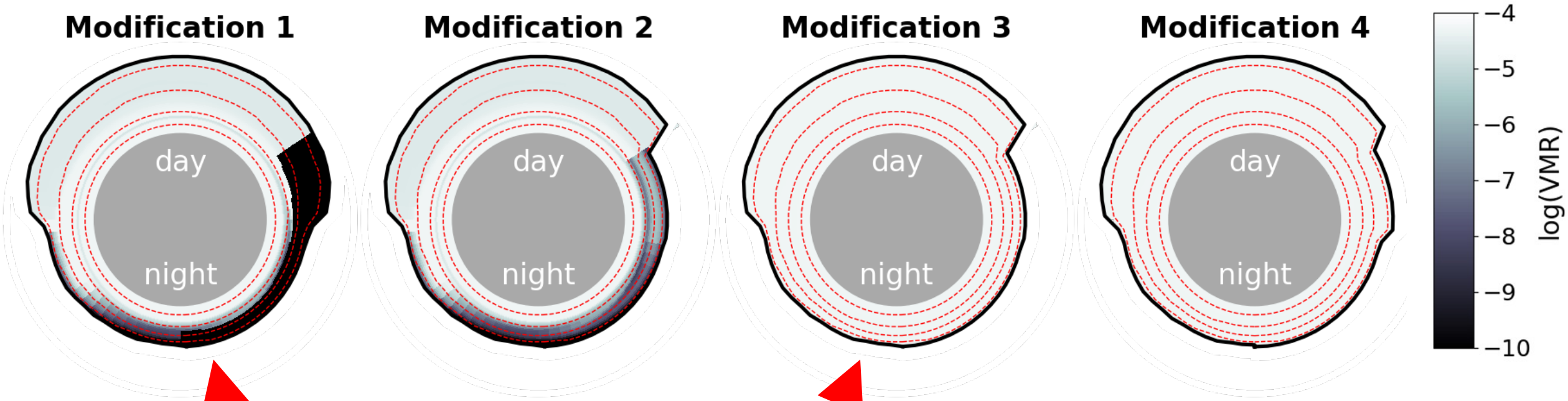

Iron removed from leading limb

Nightside temperatures on leading limb
+ uniform iron abundances

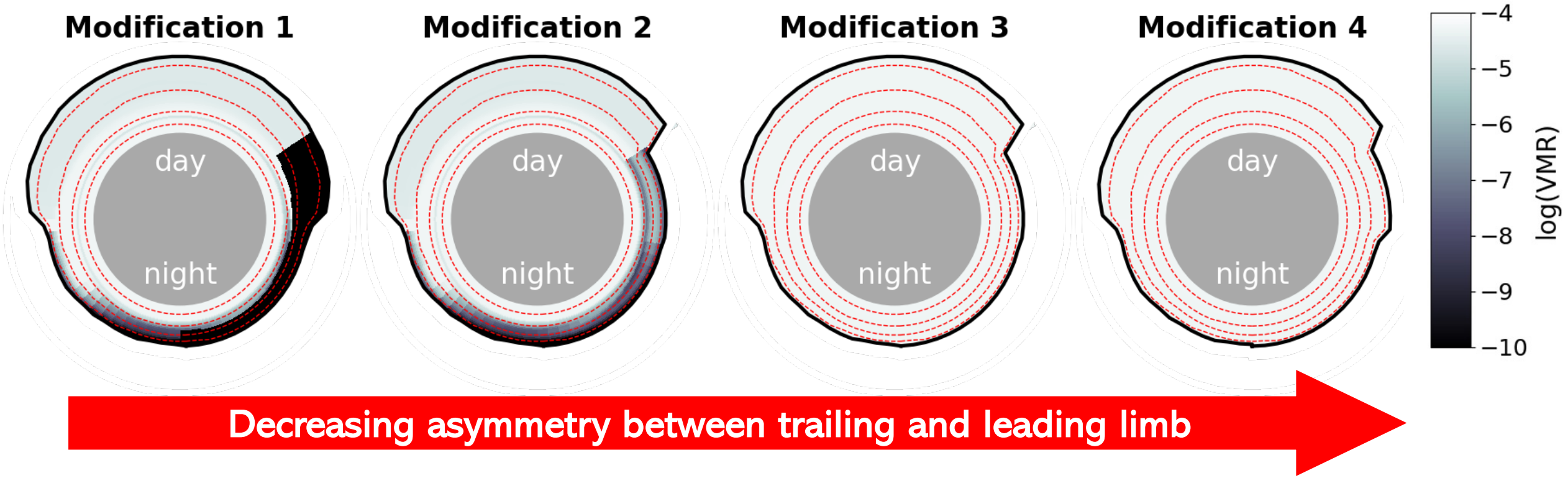
Modification 1
Modification 2
Modification 3
Modification 4
day
night
day
night
day
night
day
night
−4
−5
−6
−7
−8
−9
−10
log(VMR)
Decreasing asymmetry between trailing and leading limb

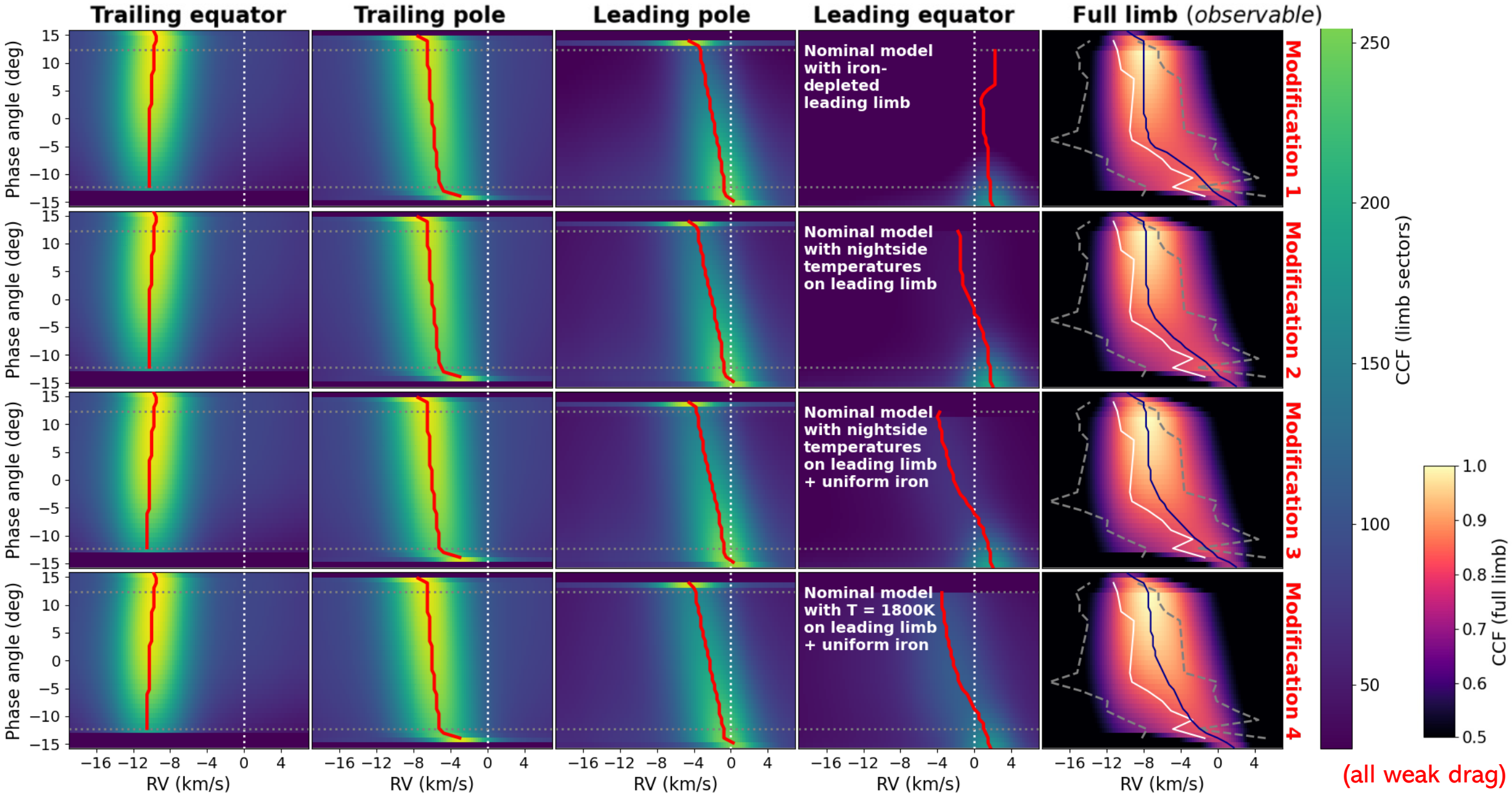
Trailing equator
Trailing pole
Leading pole
Leading equator
Full limb (observable)
Phase angle (deg)
RV (km/s)
Nominal model with iron-depleted leading limb
Nominal model with nightside temperatures on leading limb
Nominal model with nightside temperatures on leading limb + uniform iron
Nominal model with T = 1800K on leading limb + uniform iron
Modification 1
Modification 2
Modification 3
Modification 4
CCF (limb sectors)
CCF (full limb)
(all weak drag)

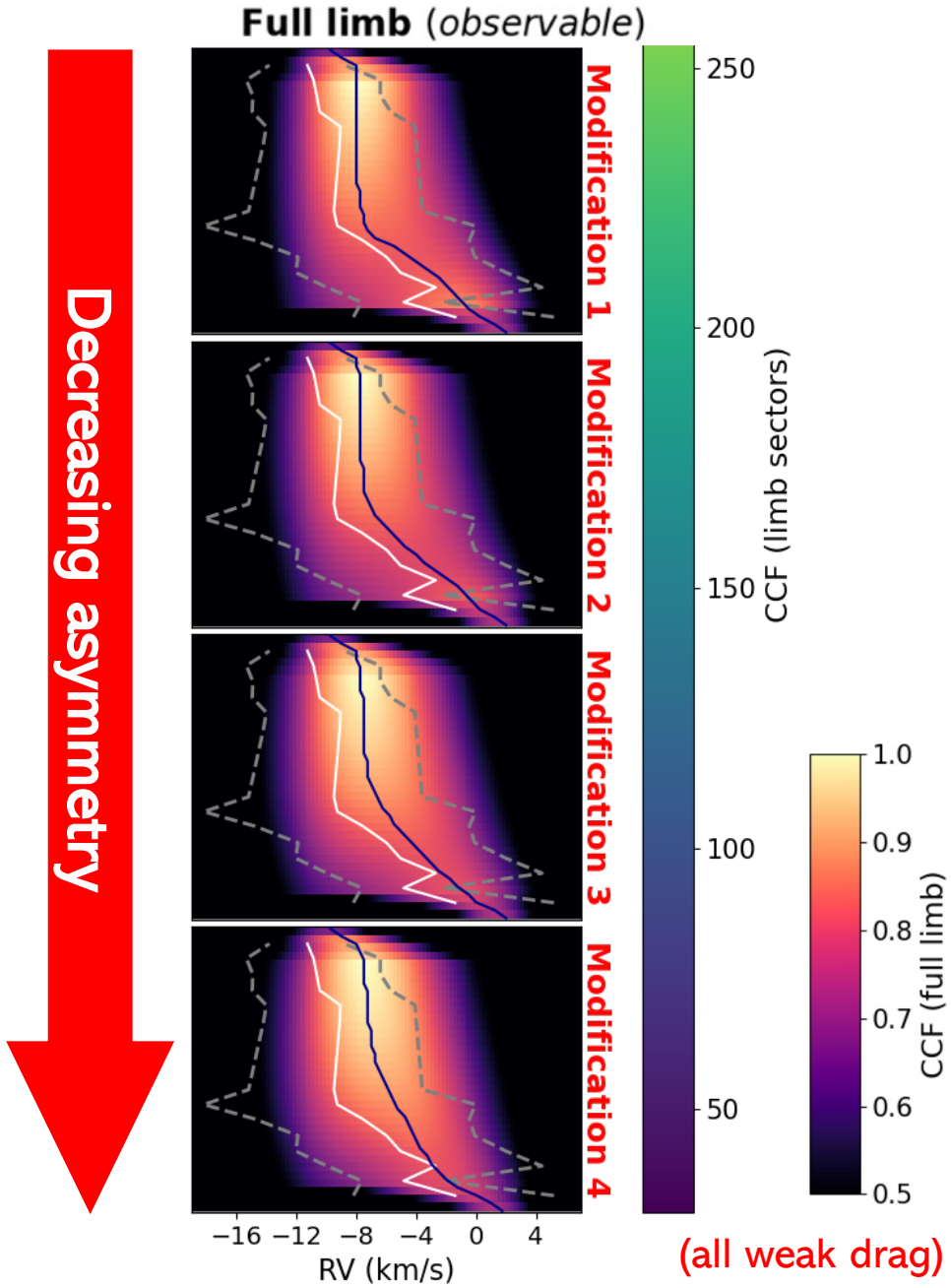
Full limb (observable)
Decreasing asymmetry
Modification 1
Modification 2
Modification 3
Modification 4
250
200
150
100
50
CCF (limb sectors)
1.0
0.9
0.8
0.7
0.6
0.5
CCF (full limb)
−16 −12 −8 −4 0 4
RV (km/s)
(all weak drag)

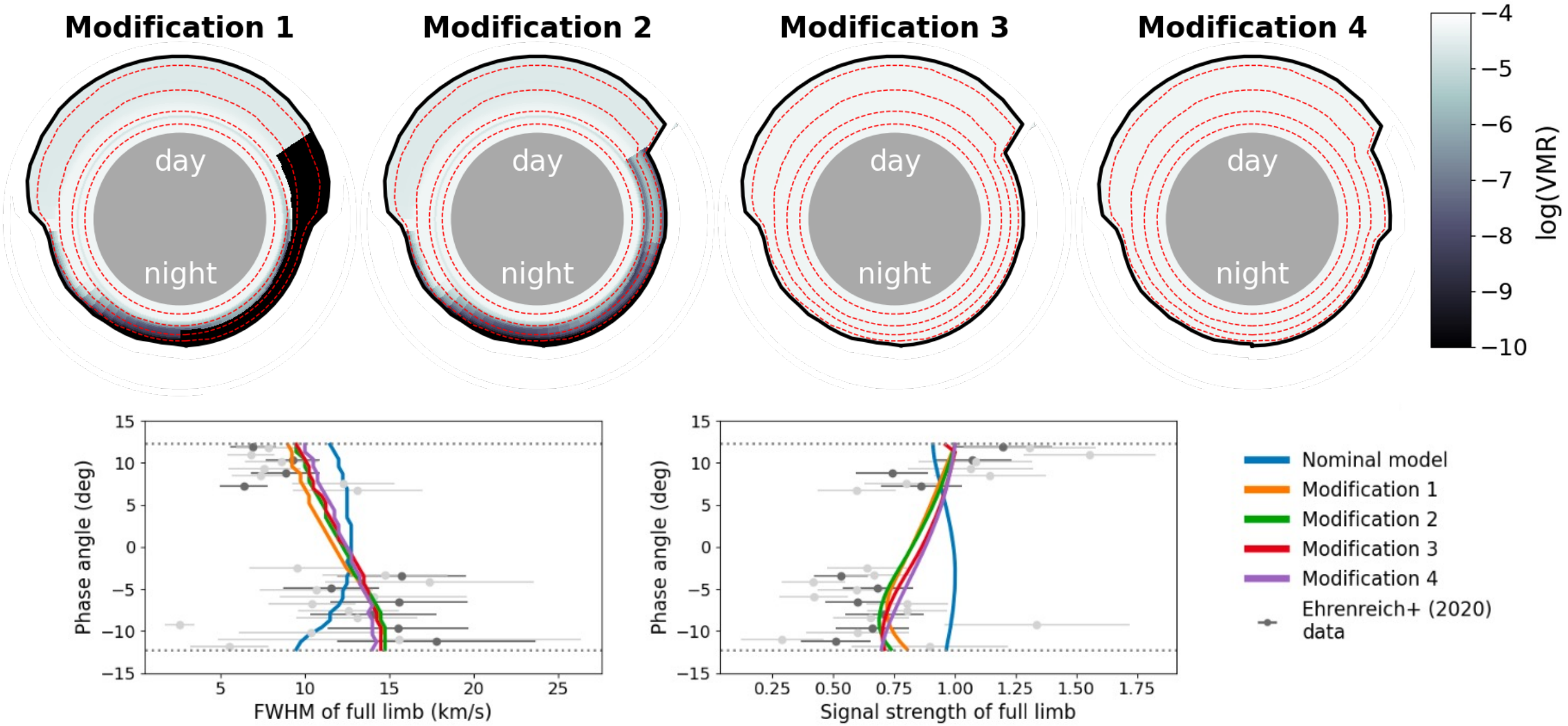
Modification 1
Modification 2
Modification 3
Modification 4
day
night
log(VMR)
−4
−5
−6
−7
−8
−9
−10
Phase angle (deg)
FWHM of full limb (km/s)
Signal strength of full limb
Nominal model
Modification 1
Modification 2
Modification 3
Modification 4
Ehrenreich+ (2020) data

From Cross-Correlation to K_p-V_{sys} Map

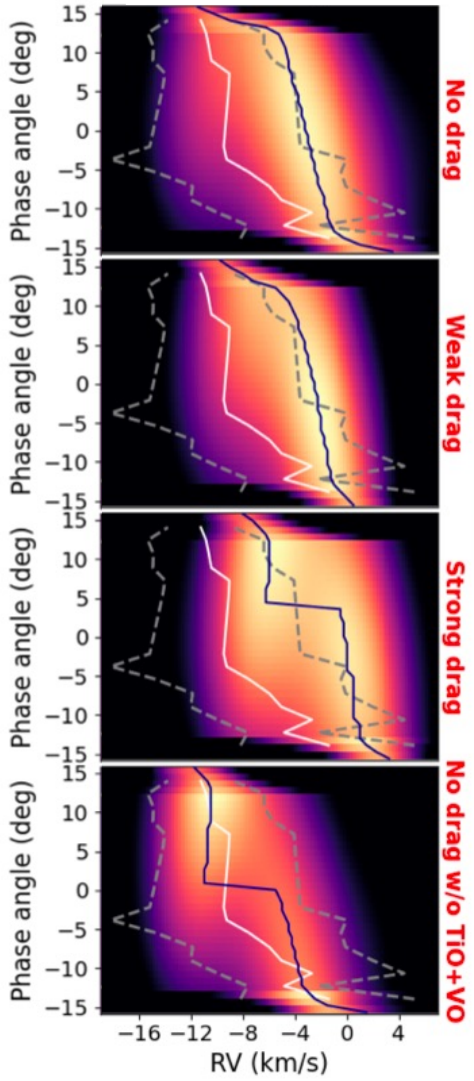

From Cross-Correlation to K_p-V_{sys} Map

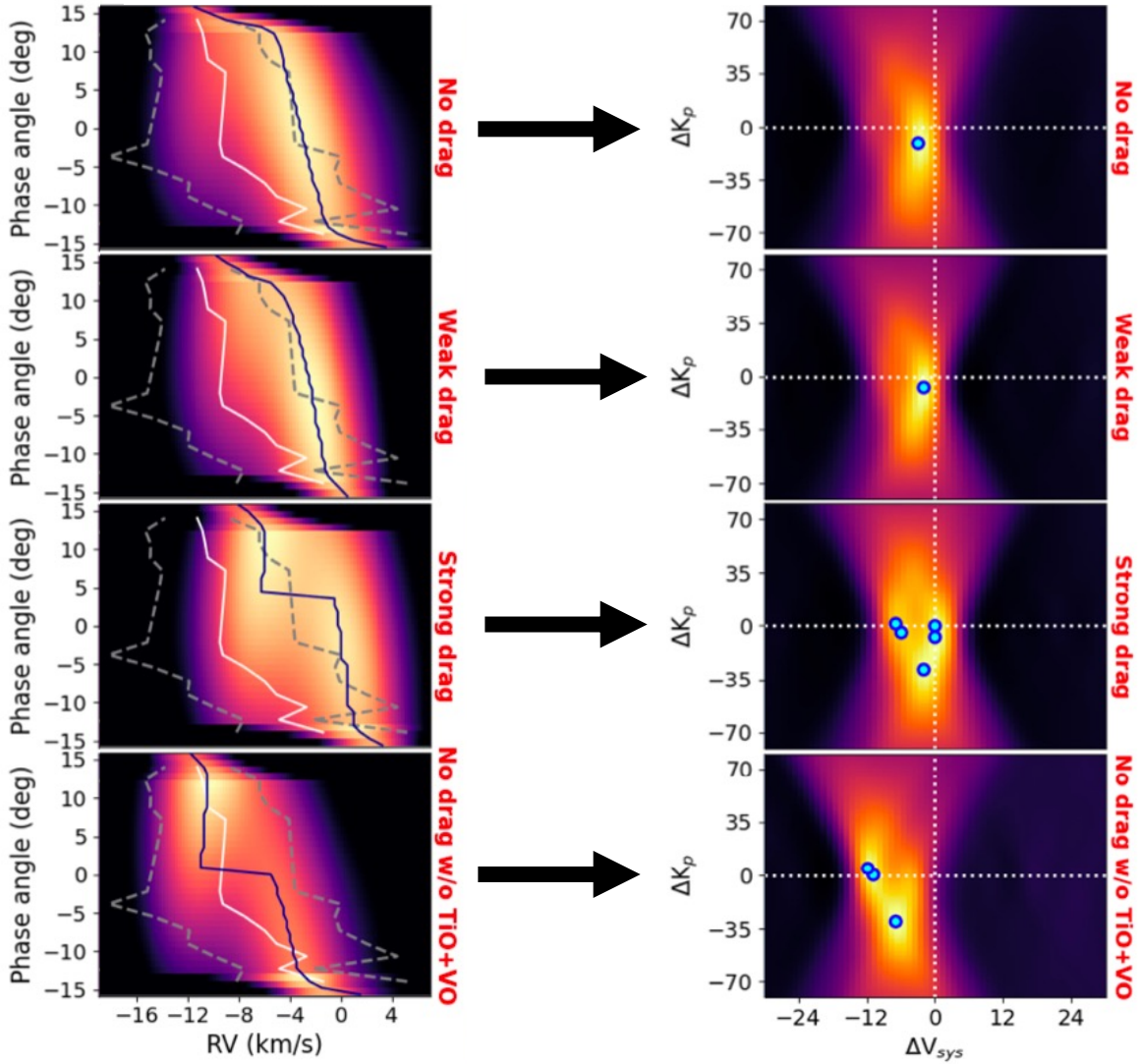

See Bibi Prinoth's talk for further details about the CCF → K_p-V_{sys} mapping

From Cross-Correlation to K_p-V_{sys} Map

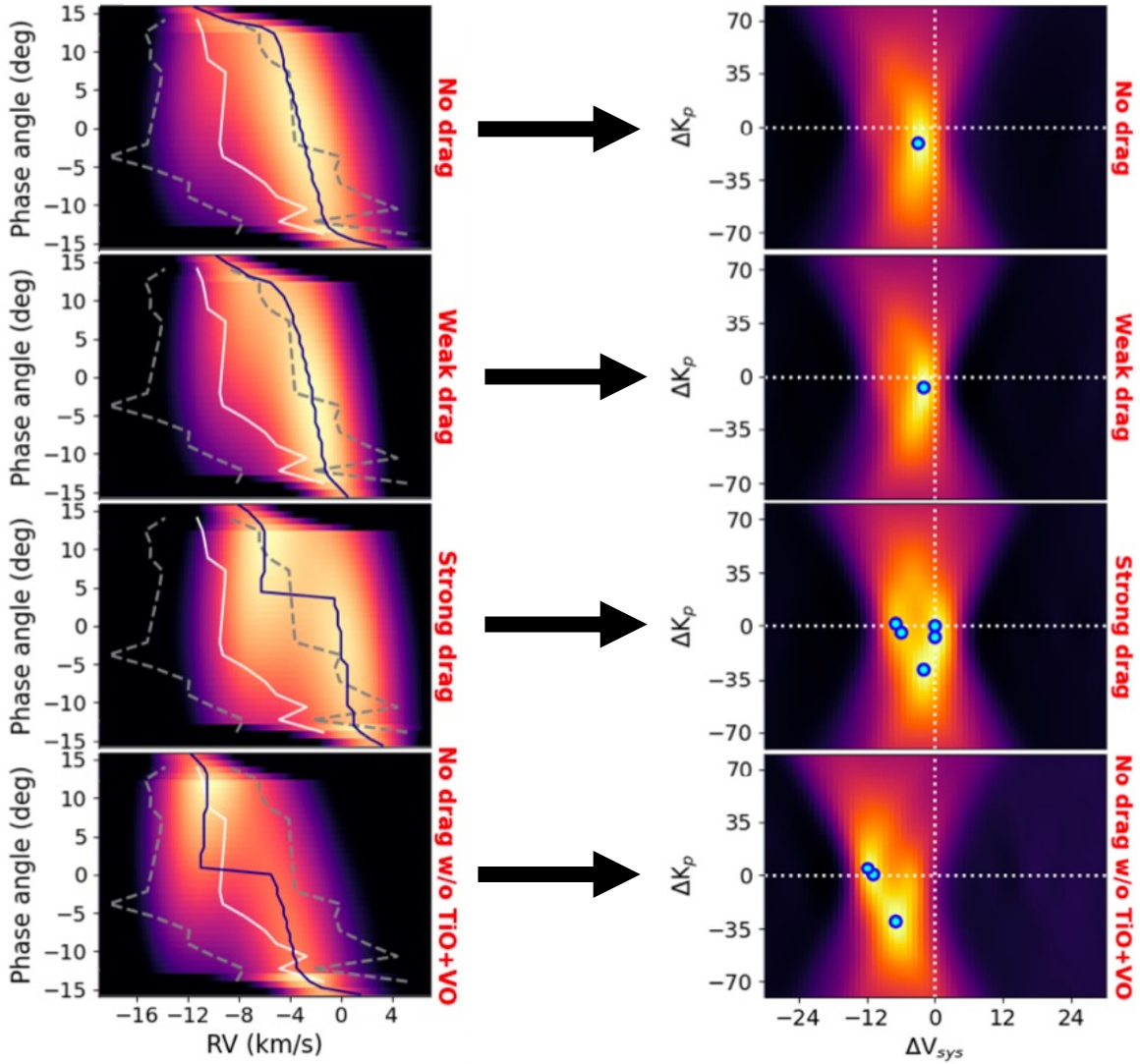

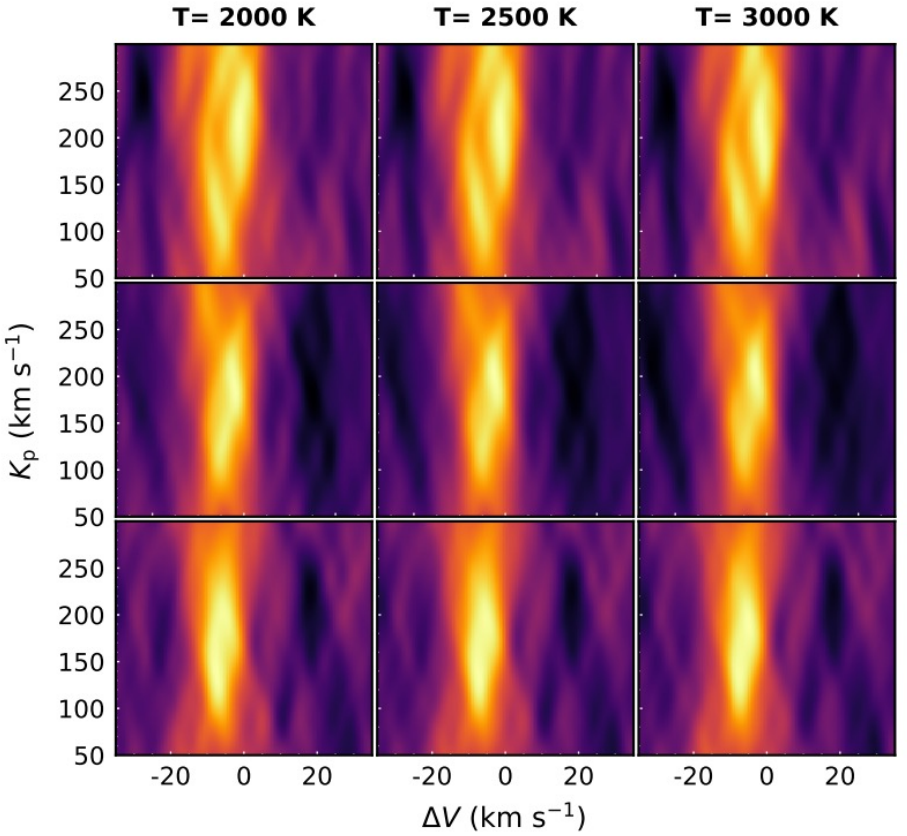

Nugroho+ 2020 (KELT-20b/MASCARA-2b)

See Bibi Prinoth's talk for further details about the CCF → K_p-V_{sys} mapping

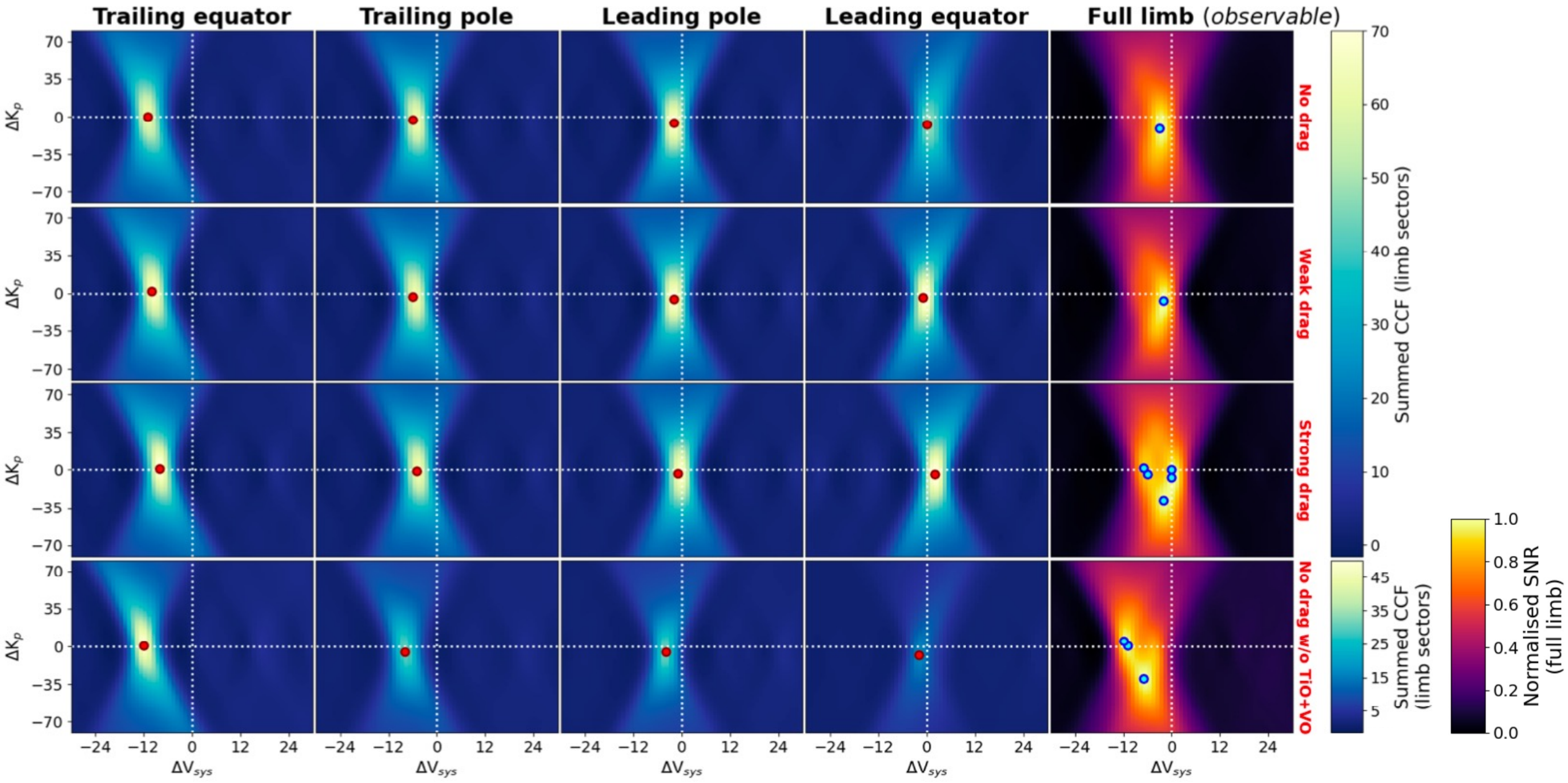
Trailing equator
Trailing pole
Leading pole
Leading equator
Full limb (observable)
No drag
Weak drag
Strong drag
No drag w/o TiO+VO
ΔKp
ΔVsys
Summed CCF (limb sectors)
Summed CCF (limb sectors)
Normalised SNR (full limb)

Summary & Conclusion

- Interpreting high-resolution spectra of ultra-hot Jupiters requires models that can account for 3D effects
- The iron signal of WASP-76b suggests a strong chemical or thermal asymmetry between the trailing and leading limb
- The cross-correlation and K_p–V_{sys} maps of the full limb can be decomposed into contributions from different limb sectors

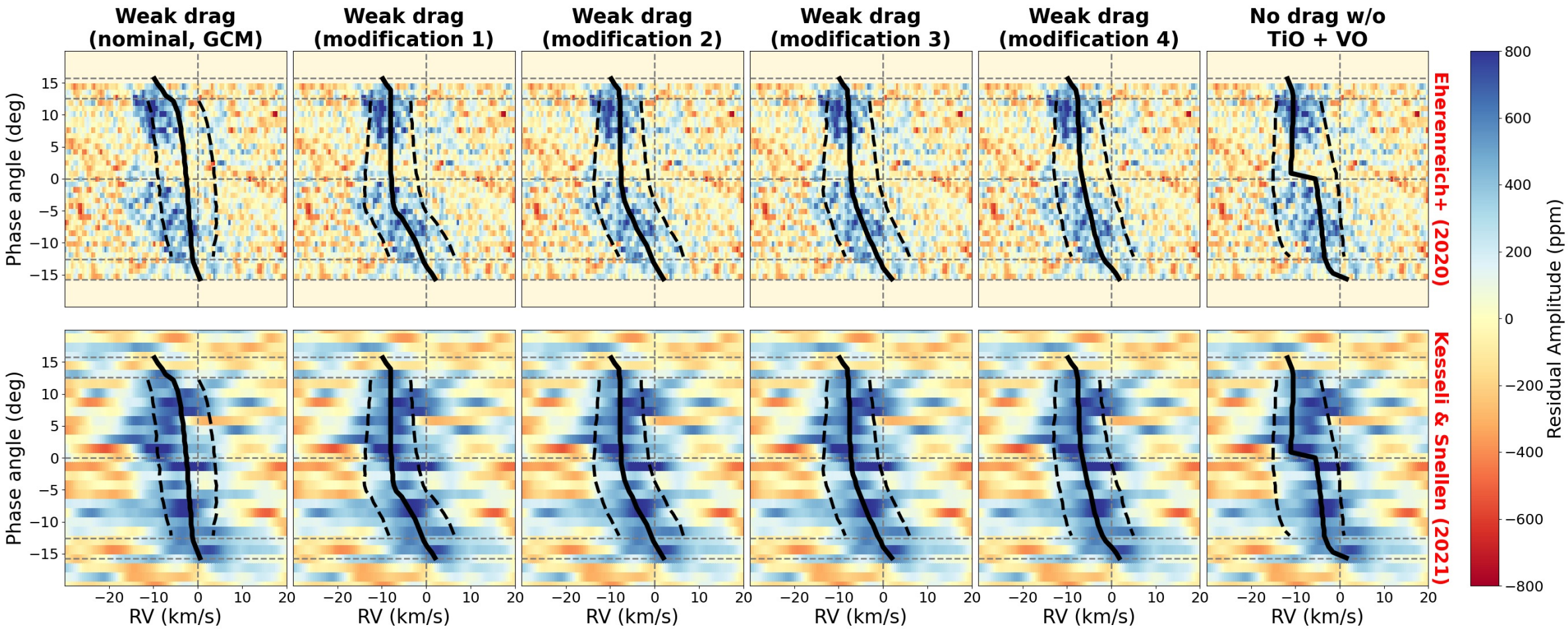
Weak drag (nominal, GCM)
Weak drag (modification 1)
Weak drag (modification 2)
Weak drag (modification 3)
Weak drag (modification 4)
No drag w/o TiO + VO
Phase angle (deg)
RV (km/s)
Eherenreich+ (2020)
Kesseli & Snellen (2021)
Residual Amplitude (ppm)